Disentangling thermal and compositional effects on β relaxation in metallic glasses

Dazhe Xu,[1,*] Zhi Chen,[1,2,*] Hongbo Lou,[1,*] Songyi Chen,[1] Ziliang Yin,[1] Ye Liu,[1] Xiehang Chen,[1] Fujun Lan,[1] Xin Zhang,[1] Zhidan Zeng,[1] and Qiaoshi Zeng[1,3,†]

[1]*Center for High Pressure Science and Technology Advanced Research, Shanghai 201203, China*

[2]*Jiangsu Key Laboratory of Advanced Metallic Materials, School of Materials Science and Engineering, Southeast University, Nanjing 211189, China*

[3]*Shanghai Key Laboratory of Material Frontiers Research in Extreme Environments (MFree), Shanghai Advanced Research in Physical Sciences (SHARPS), Shanghai 201203, China*

(Received 7 January 2025; accepted 30 October 2025; published 17 November 2025)

β relaxation is a key dynamic feature of glasses, influencing a wide range of properties. Although many factors, such as thermal history and composition, have been extensively studied and reported to significantly influence β relaxation, considerable controversy persists, limiting a deeper understanding of β relaxation in glasses. Here, we employ a binary metallic glass (MG), $Ce_{75}Al_{25}$, as a model system with a polymorphic crystallization process to minimize thermally induced compositional deviations. This enables us to separate and analyze the thermal and compositional impacts on β relaxation using dynamic mechanical analysis (DMA) across various thermal annealing treatments below the glass transition temperature (T_g) and above the crystallization temperature (T_x). We clarify that relaxation dynamics at temperatures not far below T_g are primarily governed by α relaxation, and changes to the energy states of glasses (or atomic structures) through sub-T_g annealing have minimal impact on β relaxation signals. These findings suggest that the β relaxation of $Ce_{75}Al_{25}$ MG is in fact a pseudo Johari-Goldstein (JG) relaxation rather than a genuine JG β relaxation. It is suggested that β relaxation behaves more like a localized dynamic event involving only a fraction of atoms, which may aid in crystallization nucleation below T_g. By contrasting the effects of thermal annealing on other Ce-Al binary MGs with primary crystallization processes, we further reveal that the position of β relaxation is primarily composition-dependent. These results shed new light on the thermal and compositional effects on β relaxation in MGs.

DOI: 10.1103/1b87-ycj2

I. INTRODUCTION

Generally, glass is in a nonequilibrium and thermodynamically metastable state, with excess Gibbs free energy compared with its stable crystalline counterpart. Thus a glass system will continuously evolve with time via relaxation processes towards more stable configurations, and eventually crystallization may set in on sufficiently long timescales. Therefore, in principle, the structure and properties of glasses are strongly dependent on thermal history and significantly influenced by relaxation dynamics. The glass relaxation spectrum spans tens of orders of magnitude in time and exhibits very complex patterns, which are believed to hold the key to understanding and controlling glass states and remain a central challenge in glass science [1].

In metallic glasses (MGs), the primary relaxation process accessible at temperatures well below the glass transition temperature (T_g) is usually observed as a peak, shoulder, or excess wing of the loss modulus spectra measured by mechanical spectroscopy [2–6], corresponding to the secondary relaxation event, so-called β relaxation. The origin of β relaxation, its controlling factors, and its relationship with glass structure, properties, and behaviors have attracted extensive research interest but remain elusive, with many controversial issues [1].

Numerous studies of the thermal histories and aging effects on β relaxation in glasses have revealed intriguing yet highly diverse behaviors. For example, in MGs, aging and relatively slow melt-quenching reduce the intensity or shift the position of β relaxation but cannot totally suppress it [7,8], similar to the observations in molecular glass formers [9–13]. However, in some polymer glasses, β relaxation is not affected by thermal histories or physical aging below T_g [14–16]. Ngai proposed classifying β relaxation into genuine Johari-Goldstein (JG) and pseudo JG β relaxation, with the former strongly influenced by thermal history and the latter showing minor sensitivity [17]. In addition, β relaxation is believed to drive structural changes deep in the glassy state during aging, since the primary relaxation mode (α relaxation), referring to the escape of atoms from their nearest-neighbor cage that enables large-scale structural reorganization and flow, is "frozen" below T_g [1]. In contrast, some glass formers show that aging dynamics are always dominated by the structural α-process [13,18]. Furthermore, Sun *et al.* reported that aging dynamics below T_g in MGs are independent of β relaxation and instead show a stretched exponential decay with a universal stretching exponent of 3/7 [19].

Crystallization not only competes with the glass formation during melt quenching but can also occur after glass formation

*These authors contributed equally to this work.
†Contact author: zengqs@hpstar.ac.cn

as a slow yet spontaneous destabilization process via relaxation [20]. Therefore crystallization is well recognized to be closely linked with relaxation processes in glasses [21–23]. Controlled crystallization of MGs can enhance their mechanical [24,25], magnetic properties [26], and catalytic properties [27]. Therefore understanding and controlling crystallization in metastable MGs are of great importance. According to Oguni *et al.* [28–30], in the rigid glass structure, it is believed that β relaxation leads to nucleation or crystal embryo formation [31]. Consistent with this, studies in MGs show that perturbations from external periodic fields markedly accelerated crystallization below T_g, attributed to the accumulation of atomic jumps associated with β relaxation being stochastically resonant with ultrasonic vibrations [32,33]. Moreover, Song *et al.* suggest that β relaxation can persist into the supercooled liquid state at high temperatures and may even suppress nucleation of crystals [34]. Therefore the relationship between crystallization and β relaxation in MGs remains far from well understood and calls for further efforts.

The behaviors of β relaxation in MGs are also significantly influenced by composition, owing to differences in mixing enthalpy between constituent elements. As a result, MGs exhibit distinct β relaxation characteristics, peaks, shoulders, or excess wings in relaxation spectra [35,36]. Excluding compositional effect is therefore essential for clarifying the structure and energy states related to the mechanism underlying glass relaxation. For most of the MGs with complex compositions, multiple phases typically form upon crystallization, indicating a strong thermodynamic driving force for the tendency of compositional fluctuation or separation during annealing. However, in certain polymorphic systems, such as $Ce_{75}Al_{25}$ MG, crystallization occurs via polymorphic transitions into Ce_3Al crystals through thermal annealing (hexagonal-Ce_3Al) or cold-compression (fcc-Ce_3Al) [37–39] without compositional variation relative to the initial glass matrix, namely, via a polymorphic process. Therefore, in this work, we have chosen the simple binary polymorphic system, $Ce_{75}Al_{25}$ MG, as a unique model system.

In previous studies, it was reported that T_g and the β relaxation signals were undetectable in $Ce_{75}Al_{25}$ MG using conventional differential scanning calorimetry (DSC) and dynamic mechanical analysis (DMA) [36]. Surprisingly, in this work, we identify a prominent β relaxation peak in dynamic mechanical spectroscopy (DMS) after properly annealing the as-cast samples. Without the confounding influence of thermally induced compositional fluctuations or separation, $Ce_{75}Al_{25}$ provides an ideal platform for investigating β relaxation under different energy states (atomic structures) induced by various thermal treatments. We demonstrate that β relaxation in $Ce_{75}Al_{25}$ MG remains almost unchanged across various thermal histories, whereas aging dynamics below T_g are dominated by α relaxation. Moreover, the β relaxation peak in partially crystallized $Ce_{75}Al_{25}$ MG composites becomes even more separated, but with almost constant peak position, distinguishing $Ce_{75}Al_{25}$ MG from other Ce-Al and most other MGs. This indicates that the commonly observed thermal-history-dependent shifts in β relaxation peak position likely originate from thermally induced compositional variations in MGs. We also clarify that crystallizations induced by annealing below and above T_g, exert opposite influences on β relaxation. Thus, by employing $Ce_{75}Al_{25}$ MG with polymorphic crystallization, we exclude the confounding effects of compositional fluctuations and resolve the elusive behavior of β relaxation, its relationship with thermal history, crystallization, and structure. By demonstrating that the intrinsic β relaxation is thermally stable and that its commonly observed peak shifts originate from extrinsic compositional variations, it challenges the prevailing view that directly links β relaxation dynamics to the local structural order of the glassy matrix. This study establishes a critical paradigm for disentangling intrinsic relaxation physics from extrinsic effects, providing a new theoretical framework for understanding the structure-dynamics relationship in amorphous materials.

II. MATERIALS AND METHODS

Sample preparation and characterization. Master alloy ingots with the nominal composition of $Ce_{75}Al_{25}$ were prepared by arc-melting of high-purity elements (>99.9 at.%) in a Ti-gettered high-purity argon (Ar) atmosphere. The ingots were re-melted at least four times to ensure chemical homogeneity. $Ce_{75}Al_{25}$ ribbons with a thickness of ~15 μm were produced by the melt-spinning method with a single copper roller in a high-purity Ar atmosphere. The fully amorphous nature of the as-cast MG ribbons was verified by synchrotron XRD at the beamline BL15U1 of Shanghai Synchrotron Radiation Facility (SSRF), China, and DSC (Perkin-Elmer 8500), as shown in Fig. 1.

DMA measurement. DMS spectra were collected on a DMA (TA Discovery 850) in the film tension mode. Tests were carried out in tensile geometry with a preload (static force) of 0.08 N. The relative strain amplitude (ε) was 5×10^{-4} for each sample. The temperature ramp was set with a heating rate of 3 K/min. To prevent oxidation at elevated temperatures, samples were measured under flowing ultrahigh-purity N_2 gas.

III. RESULTS

A. β relaxation in the $Ce_{75}Al_{25}$ MG

Figure 2(a) shows the normalized loss modulus of the as-cast $Ce_{75}Al_{25}$ MG and samples annealed at different temperatures. The as-cast sample shows a clear shoulder from 325 to 420 K (centered at ~370 K), which likely corresponds to a typical β-relaxation process. However, the intensity of this shoulder decreases rapidly with increasing annealing temperature. As shown in the inset of Fig. 2(a), a corresponding hump appears in the storage modulus of the as-cast MG, inconsistent with the hollow feature of a typical β relaxation. Such a pronounced annealing effect on the sub-T_g shoulder in DMS has been reported before in other MG systems [40–42] and was attributed to the release of internal stress (quenched-in local stress fluctuations) or relaxation of excess enthalpy upon heating, rather than a reversible β-relaxation process.

Figure 2(b) presents the evolution of loss modulus (E'') from 253 to 383 K during successive continuous heating cycles of $Ce_{75}Al_{25}$ MG. The first heating to 383 K, followed by a five-minute hold, is designed to release internal stress or relax excess enthalpy in the as-cast MGs. Consequently, the second heating curve (red symbol) corresponds to a more

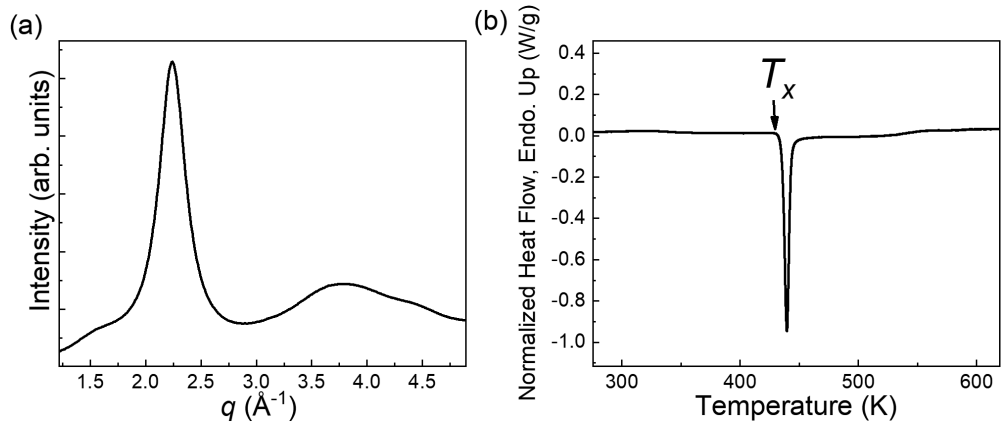

FIG. 1. Characterization of glassy features of $Ce_{75}Al_{25}$ metallic glass ribbon. (a) Synchrotron XRD reveals a typical amorphous peak. (b) DSC trace determining the crystallization temperatures (T_x).

stable state, closer to equilibrium. A prominent peak/hump emerges at ∼300 K after the first heating, barely visible in the as-cast sample, and the third heating (blue symbol) curve nearly coincides with the second one, demonstrating the reproducibility of this feature. This indicates that the process associated with the peak/hump at ∼300 K is reversible after annealing at 383 K, suggesting a β-relaxation process that might be only visible when the sample's excess enthalpy and or internal stress are well released by annealing. The sample's amorphous nature after annealing was confirmed by XRD and DSC measurements. Hereafter, we defined this 383 K annealed state as the well relaxed "standard" state of $Ce_{75}Al_{25}$ MG for better comparison.

Figure 3 shows the loss modulus (E'') and storage modulus (E') of the annealed "standard" $Ce_{75}Al_{25}$ MG measured at the frequency (f) of 0.1 Hz from 200 to 510 K. Similar to other rare earth elements-based binary MGs [36], $Ce_{75}Al_{25}$ crystallizes almost simultaneously with the glass transition. Thus the primary E'' peaklike shape corresponds to the low-temperature tail of the alpha relaxation cut by the onset of crystallization. The peak at ∼300 K on E'' matches well with the drop on E', which further supports its assignment to β relaxation. The dynamic modulus data were fitted with the Havriliak-Negami (H-N) function [43] in the temperature (T) domain:

$$E^*(f) = E_{\beta(\alpha)\infty} + [E_{\beta(\alpha)0} - E_{\beta(\alpha)\infty}] \times \left[1 + (i2\pi f \tau_{\beta(\alpha)})^{a_{\beta(\alpha)}}\right]^{-b_{\beta(\alpha)}}, \quad (1)$$

where $E_{\beta\ (\alpha)\ 0}$ and $E_{\beta\ (\alpha)\ \infty}$ are the equilibrium and instantaneous moduli of the MG in the T range of β (or α) relaxations, respectively. The parameters a and b are the shape factors ($0 \leqslant a, b \leqslant 1$) and for β relaxation, $b_\beta = 1$ corresponding to the Cole-Cole equation. The relaxation time τ_β of β relaxation can be expressed by the Arrhenius equation $\tau_\beta = \tau_{0\beta} e^{E_\beta/RT}$, where $\tau_{0\beta}$ is the attempt relaxation time of β relaxation, E_β is the activation energy, and R is the universal gas constant [44,45]. The relaxation time τ_α of α relaxation can be expressed with the Vogel-Fulcher-Tammann (VFT) equation $\tau_\alpha = \tau_{0\alpha} e^{DT_0/(T-T_0)}$, where $\tau_{0\alpha}$ is the attempt relaxation time of α relaxation and D is the fragility factor [46,47]. The green solid curve shown in Fig. 3 is the fitting result of the coupled relaxation processes from 273 K to 413 K in the E'' spectrum with the above equations, which consists of the

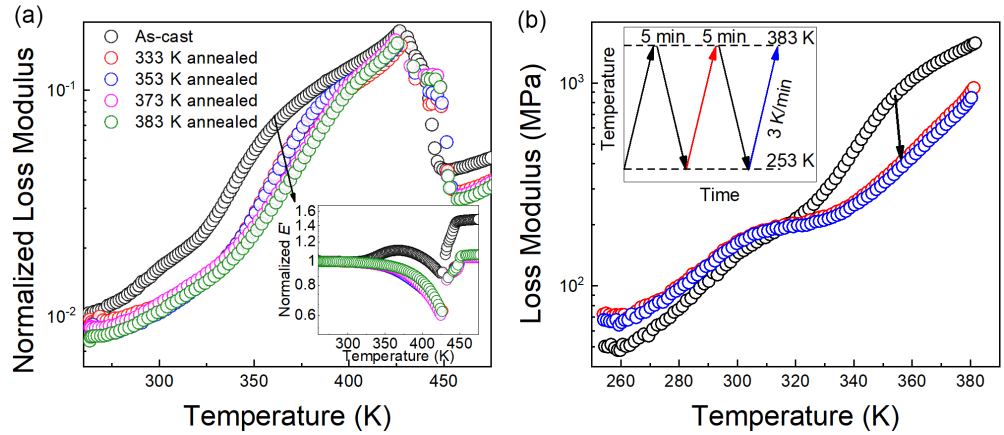

FIG. 2. Annealing effects on the temperature dependence of the mechanical spectrum in a $Ce_{75}Al_{25}$ metallic glass. (a) Normalized loss modulus (normalized by unrelaxed modulus, i.e., storage modulus at low temperature) of as-cast MG and samples annealed at different temperatures. The inset shows the corresponding normalized storage modulus. (b) Evolution of loss modulus during successive continuous heating processes. The inset shows a schematic illustration of the DMA experiment.

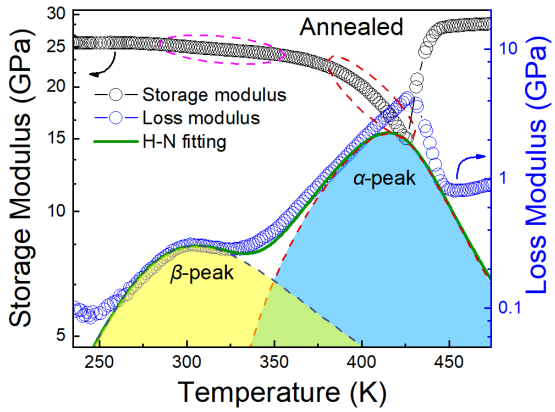

FIG. 3. Temperature dependence of storage modulus and loss modulus in an annealed $Ce_{75}Al_{25}$ metallic glass (383 K annealed for 5 min, heating rate: 3 K/min, and driving frequency: 0.1 Hz). The green solid line is the H-N fit of the relaxation spectrum, which is a combination of α relaxation (red dotted line and blue region) and β relaxation (blue dotted line and yellow region). The drop in storage modulus at ~300 K, corresponding to the β relaxation, is highlighted by the purple dotted ellipse.

β- and α-relaxation peaks represented as yellow and blue regions, respectively. The fit parameter, E_β, is obtained to be 118.7 ± 0.9 kJ/mol.

B. Thermal effects on β relaxation

Figures 4(a) and 4(b) show E'' and E' of the as-cast and relaxed "standard" $Ce_{75}Al_{25}$ MGs, obtained from multi-frequency measurements from 253 K to 453 K with a temperature step of 5 K. Because the heating rates in these measurements can be much lower than 3 K/min in these isochronal tests, an obvious temperature shift of DMS would be expected. In the as-cast sample E'', the low-temperature β-relaxation peak and the subsequent enthalpy relaxation shoulder gradually merged into a faint shoulder as the frequency increases, resulting from their different frequency dependence. The master curves shown in Fig. 4(c) were constructed using the time-temperature superposition (TTS) principle [48,49], which predicts the viscoelastic behaviour of glass across a broad range of frequencies or timescales by combining data obtained at different temperatures. The relaxation time versus temperature can be represented by the shift factor, α_T, from TTS, i.e., $\tau(T) = \alpha_T \tau(T_{\text{ref}})$ [50], plotted in Fig. 4(d). The activation energies of β relaxation (E_β) of the two states can be obtained by the Arrhenius equation [51]. The fit result of E_β for the annealed state marked in Fig. 4(d) agrees well with the result from H-N fitting in Fig. 3.

Figure 5(a) shows E'' of the $Ce_{75}Al_{25}$ MG in different states, which are also normalized by the unrelaxed modulus. It can be seen that E'' signal of the long-time aged $Ce_{75}Al_{25}$ MG (~4 years at 233 K) is similar to that of the "standard" MG in the temperature range from ~250 to ~380 K shown in Fig. 2(b). The β relaxation becomes an even more pronounced peak when the aged sample is further annealed with the same annealing protocol in Fig. 2(b). Further cold-rolling with ~21% reduction of the ribbon thickness leads to the recovery of the dynamical behavior back to a state similar to the previous long-time aged one (~4 years at 233 K). These results further confirmed that the β relaxation signal would be more pronounced if excess enthalpy is well relaxed by aging, and plastic deformation by cold-rolling could not further enhance it. In Fig. 5(b), using the sample aged at 233 K for ~4 years and then annealed at 383 K for 5 minutes as the reference state (green solid line), which is closest to the equilibrium state, the normalized E'' of other states are subtracted from the reference state (dotted lines) to present the changes associated with the different treatments. It is evident that structural or energy tuning induced by annealing or plastic deformation (cold-rolling) here mainly affects the high-temperature tail of the α relaxation (blue region), while the low-temperature side of the β relaxation peak (yellow region) is barely affected. Generally, cold-rolling rejuvenates MGs by increasing enthalpy and structural disorder, resulting in an increase in the concentration of quasipoint defects (QPD) according to the QPD theory [52]. Such increases are typically expected to enhance β relaxation. The seemingly decoupling between QPD concentration and the strength of the β-relaxation peak observed in this work is therefore surprising and warrants future investigation.

To further identify which relaxation process dominates during physical aging below or near T_g, isothermal aging experiments were performed at different temperatures in the glassy state. Fig. 6 shows the loss modulus at five different isothermal aging temperatures as a function of aging time, normalized by the initial values E'' ($t = 0$). The E'' clearly deviates from a simple exponential decay and can be described by a stretched exponential function [13]:

$$\frac{E''(t)}{E''(t=0)} = \left\{ \Delta E''(t) \exp\left[-\left(\frac{t}{\tau_{ag}} \right)^{\beta_{ag}} \right] + E''_{\text{eq}} \right\} \Big/ E''(t=0), \tag{2}$$

where $E''_{\text{eq}} \equiv E''(t \to \infty)$ is the equilibrium value, $\Delta E''(t)$ is the change during aging ($\Delta E''(t) = E''(t=0) - E''_{\text{eq}}$), β_{ag} is the stretching exponent, and τ_{ag} is a constant of the aging (or decay) time. The best fits of Eq. (2) are displayed in Fig. 6 as solid lines. All aging curves at different temperatures collapse onto one single master curve (inset of Fig. 6), when shifted according to TTS. The TTS principle is based on the idea that increasing temperature has a similar effect to decreasing frequency or increasing time. Thus the aging curves share a similar shape factor, and the stretching exponent was assumed to be fixed at $\beta_{ag} = 0.5$, which can describe the aging processes very well [48,53]. Meanwhile, it should be noted that Eq. (2) could not describe the time dependence of $E''(t)$ for data very close to T_g due to expected variation of τ_{ag} during relaxation towards equilibrium [18]. Aging close to T_g (383 K and 373 K) cannot reach an equilibrium value, likely due to the onset of crystallization, so the long-time data ($t >\sim$ 18000 s for 373 K and $t >\sim$ 12000 s for 383 K) are excluded from analysis.

C. Crystallization effect on β relaxation

As metastable systems, crystallization is nearly inevitable when MGs are subject to long-time or high-temperature annealing. To address the influence of crystallization (or

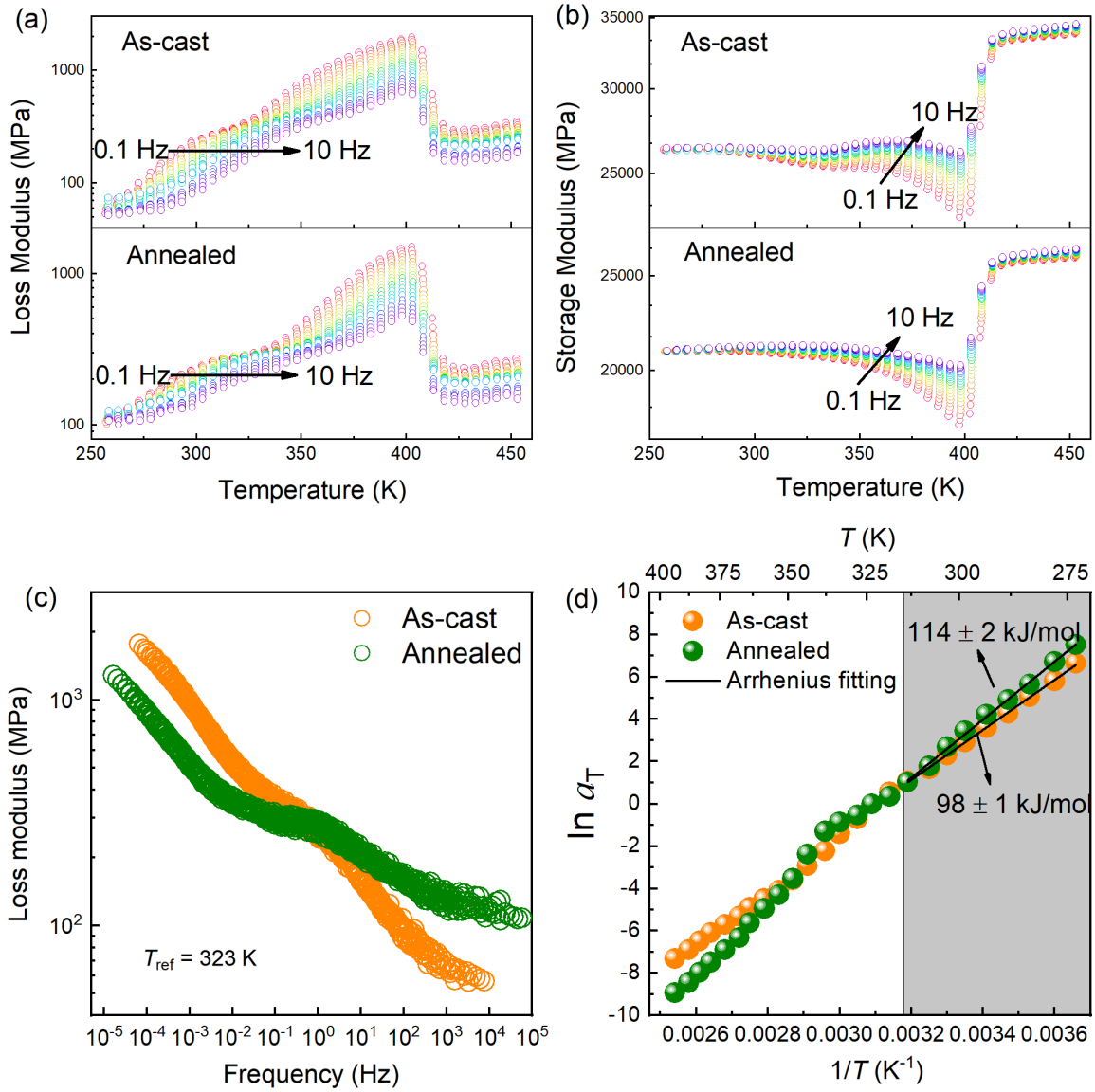

FIG. 4. Multi-frequency test results and time-temperature superposition results of as-cast and annealed $Ce_{75}Al_{25}$ MGs applying frequencies from 0.1 to 10 Hz. (a) Loss modulus. (b) Storage modulus. (c) Master curves for the loss modulus with 323 K as the reference temperature. (d) Shift factors vs temperature, the grey region is the temperature regime of β relaxation.

nanoscale nucleation or clustering) during annealing on β relaxation, we performed continuous heating and cooling experiments around or above T_g using DMA on partially-crystallized MG composites. The sample was first annealed to the relaxed "standard" state and then subjected to nine heating-cooling cycles (3 K/min, 5 min soaking time at the highest temperature). Figure 7 shows the heating data (red dots) and a nearly fully crystallized sample (blue dots). The same annealing protocols were repeated in DSC to evaluate crystallinity, as shown in Fig. S1 [54]. It is noted in Fig. 7 that the first and second heating processes to 393 K and 403 K lead to a reduction in loss modulus across almost the entire temperature range, which corresponds to ∼20% of crystalline phase volume fraction according to the area reduction of crystallization exothermal peak in DSC curves (Fig. S1 [54]). Surprisingly, a prominent β-relaxation peak remains at the same position when the crystalline phase volume fraction reaches up to ∼60% after heating to 413 K. Upon further heating to 473 K following the protocol shown in the inset of Fig. 7, the β-relaxation peak remains, although the crystallization volume fraction increases further. The α-relaxation peak shifts continuously toward higher temperatures upon heating, leading to a broadening of the overall relaxation spectrum. This broadening reflects an increase in dynamic heterogeneity, consistent with recent reports from stress relaxation measurements during aging [55]. The clearly separated α and β relaxations in $Ce_{75}Al_{25}$ MG offers a plausible explanation for the mechanism underlying this broadening in systems where the two relaxation modes are not well-resolved. The β-relaxation peak finally disappears only when the sample was annealed at a much higher temperature of 553 K for a long time, as shown in blue dots.

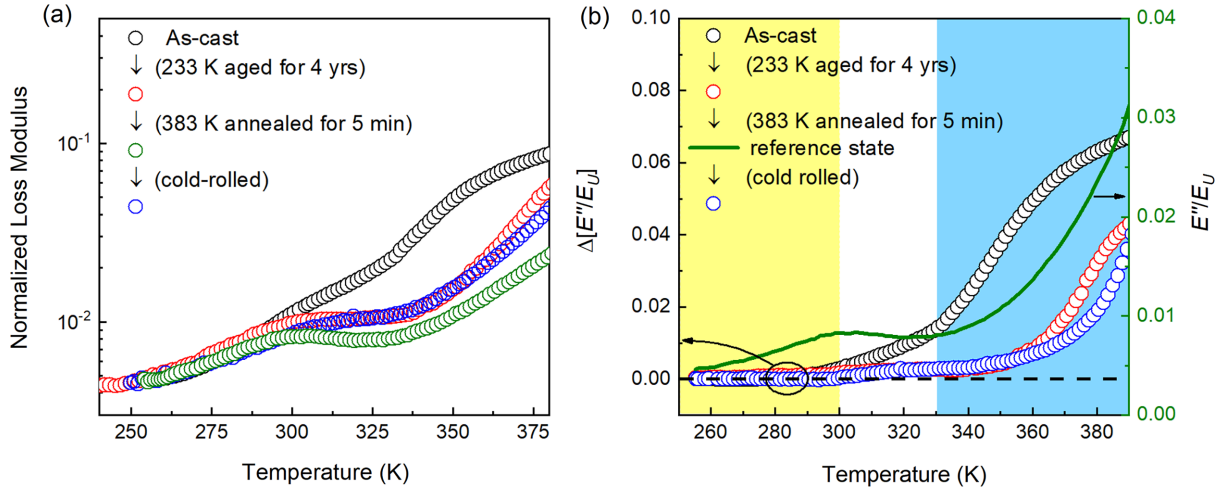

FIG. 5. Temperature dependence of normalized loss modulus for $Ce_{75}Al_{25}$ MG ribbons with different structural states. Black dot: as-cast $Ce_{75}Al_{25}$ MG. Red: MG storage at 233 K for 4 years. Green: aged sample was then annealed at 383 K for 5 min. Blue: annealed sample was then cold-rolled with 21% thickness reduction. (a) Normalized loss modulus. (b) The difference between different states, and the reference state is the ribbon after long-time low-temperature aging and short-time high-temperature annealing.

IV. DISCUSSION

A. Thermal effects

It is well known that glass relaxation dynamics and thermodynamic properties are sensitive to the thermal history of a glass [18,56]. The evolution of β relaxation in the $Ce_{75}Al_{25}$ MG with different thermal histories (energy states) is compared in Fig. 5. We note that the normalized E'' almost collapses onto one single curve on the low-temperature side of the β-relaxation peak, with the peak position nearly unchanged. In contrast, noticeable changes are present at the high-temperature side close to the α-relaxation peak region, which was often considered as aging/annealing effects on β relaxation [8,48,49,57]. In some polymers, the decrease in intensity of β-relaxation peaks can also result from the evolution of α relaxation [14–16]. To elucidate this, we followed the criteria proposed by Johari [58] to evaluate aging effects on the relaxation spectrum through variation of the spectrum between samples with different thermal histories, as shown in Fig. 5(b). It is evident that structural tuning induced here mainly affects the high-temperature tail of the α relaxation, while the low-temperature side of the β-relaxation peak is barely affected. Through scrutinizing the dynamics of an MG at the atomic length scale, it was shown that the structural relaxation strongly depends on the thermal history [59]. In previous macroscopic measurements like DMA results, these

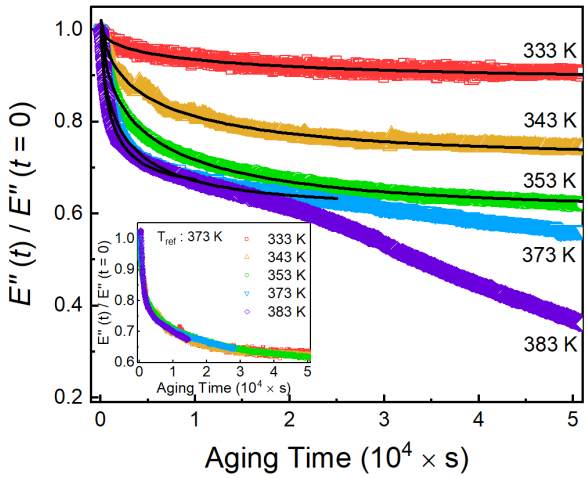

FIG. 6. Mechanical loss at $f = 0.3$ Hz vs aging time for $Ce_{75}Al_{25}$ MG at five different temperatures. The ordinate values are normalized to the value at $t_{ag} = 0$. The solid line is the fit to Eq. (2). The inset is the master curve shifted from 5 aging curves. For isothermal aging, the sample was heated from room temperature to the target aging temperature at a constant heating rate of 3 K/min with a driving frequency of 0.3 Hz. Then, the samples were held at this temperature for several hours.

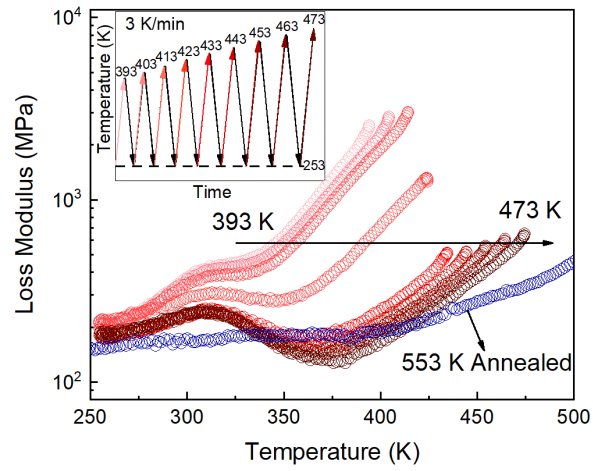

FIG. 7. Influence of partial crystallization on the β relaxation in $Ce_{75}Al_{25}$ MG. E'' vs temperature during continuous heating processes. Heating to 9 different temperatures from 393 to 473 K with the same 5 minutes soaking. The dark blue dotted line represents the totally crystallized $Ce_{75}Al_{25}$ sample obtained by annealing at 553 K for 20 min.

thermal effects were mainly reflected on the fast portions of the α relaxation, like the sub-T_g modulation results reported by Pineda *et al.* [41] and Frey *et al.* [60]. Here, the minor difference between different states on the right side of the β-relaxation peak should also result from the evolution of "background" affected by structural α relaxation associated with the release of internal stresses or annihilation of free volume [61–63].

The nearly unchanged β-relaxation peak was also observed in a significantly rejuvenated $La_{55}Ni_{20}Al_{25}$ MG after thermal cycling, while the α relaxation is clearly affected [64]. The β relaxation was also observed to be insensitive to different heat treatments below T_g in a $Pd_{42.5}Ni_{7.5}Cu_{30}P_{20}$ MG [49]. In this work, the β relaxation of the $Ce_{75}Al_{25}$ MG shows similar unchanged characteristics, i.e., the peak position and peak intensity (relaxation time and relaxation strength) are barely affected by thermal history, which conforms to the notion of pseudo-JG β relaxation clarified by Ngai and Paluch [17]. To further confirm this, other dynamic properties, for instance, the pressure dependence of β relaxation, should be investigated by experiments or simulations in the future [65,66].

In a previous work [36], the β-relaxation signal in DMS of rare earth-based binary MGs (including Ce-based ones) was found to transform from a peak to an excess wing when Ni/Co is replaced by Al, which is concordant with results of our $Ce_{75}Al_{25}$ MG before fully-annealed as shown in Fig. 2. Another similar example is that the typical excess wing in propylene carbonate (PC, $T_g \sim 159$ K) and glycerol ($T_g \sim 185$ K) develops into a shoulder during long-time aging experiments, which is attributed to different aging dependence of the α and β processes [67]. Thus we conclude that the true characteristic of β relaxation for MGs could only be reliably evaluated when the sample's excess enthalpy is well relaxed, especially for hyper-quenched glass ribbons far from their equilibrium states. (For most bulk MGs, the effects of thermal history on their intrinsic β-relaxation signal seem less critical [7,42,48,49,57,68].)

To further confirm that the aging dynamics in the $Ce_{75}Al_{25}$ MG at temperatures below T_g are dominated by α relaxation, the relaxation times of low-temperature aging (star symbols) fitted from Fig. 6 are compared with α-(triangles) and β-(sphere symbols) relaxation times, as shown in Fig. 8. The α-relaxation times are from Cole-Cole fitting parameters of multifrequency data at different temperatures, as shown in Fig. S2 [54]. The β-relaxation times are obtained from Fig. 4(d). We found that the relaxation time τ_{aging} of 383 K falls well on the VFT fit curve of τ_α. However, τ_{aging} of lower temperature aging clearly deviates from the VFT fit and is notably longer than the extrapolated τ_β, which is consistent with aging data in other molecule glasses and MGs [13,69]. The relaxation behaviour of the $Ce_{75}Al_{25}$ MG can be divided into three distinct regimes, as indicated by the dotted lines in Fig. 8. Here, we focus on identifying the dominant process in the intermediate aging regime just below T_g. To describe this glassy dynamics, we employ a modified VFT (MVFT) function [70]:

$$\tau_{\text{MVFT}} = \tau_\infty \exp\left(\frac{B}{T\left(1 - T_0/T_f\right)}\right), \tag{3}$$

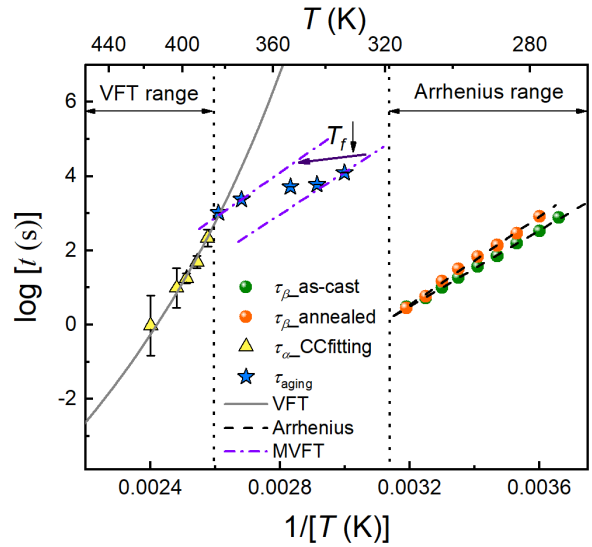

FIG. 8. Relaxation times of α process (yellow triangles) from CC fits, β process (orange and green dots) from shift factors, and aging (blue stars) from Eq. (2) fit.

where the fictive temperature T_f indicates the temperature where the observed nonequilibrium properties match the equilibrium values. This equation is widely used to model glass dynamics [13,41,71]. Applying it to the low-temperature relaxation data (Fig. 8), we find that the relaxation times fall between two MVFT fits with $T_{f1} = 398$ K and $T_{f2} = 383$ K, using the same B and T_0 parameters as in the VFT fit. We propose that as the aging temperature increases, the sample gradually approaches equilibrium, causing the fictive temperature to decrease. At $T_{\text{aging}} = T_{f2} = 383$ K, the MVFT intersects the equilibrium VFT fit. Notably, 383 K coincides with the onset temperature of macroscopic flow in DMA temperature-ramp measurements (Fig. S3 [54]), where the strain rate $d\varepsilon/dt$ of ribbon begins to deviate from zero and could serve as an indicator of the glass transition. Ultimately, the τ_{aging} at temperatures below 383 K are well described by the MVFT functions, confirming that low-temperature aging dynamics are dominated by structural α relaxation [13,18].

B. Compositional effects

Previous studies show that partial crystallization of the $La_{60}Al_{15}Ni_{25}$ MG decreases the magnitude of the entire mechanical relaxation spectrum and shifts the β-relaxation peak position [48]. This crystallization effect was ascribed to reduced atomic mobility caused by the formation of long-range order. In Fig. 7, a similar decrease in relaxation strength is also observed across the entire spectrum; however, the reduction in loss modulus is not uniform across all temperatures. The disappearance of the β-relaxation peak in the fully crystallized sample confirmed that no additional contributions to internal friction around the β-relaxation peak arise from crystalline domains in the $Ce_{75}Al_{25}$ sample.

For a more quantitative comparison, we fitted the DMS data of samples heated to 393, 403, 413, and 423 K using Eq. (1), as shown in Fig. S4 [54]. To ensure consistency, the same shape factors (a_α, b_α, a_β, and b_β) obtained from the

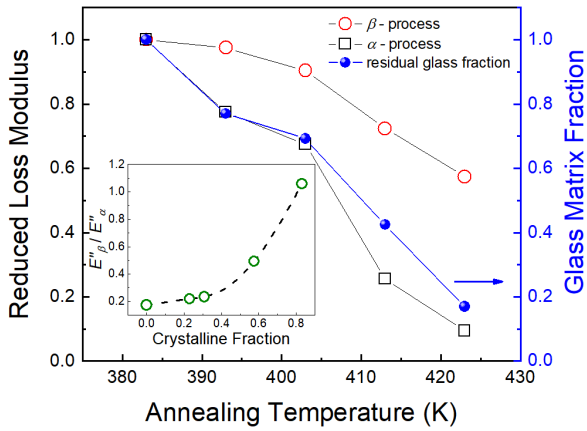

FIG. 9. The residual glass matrix fraction and reduced loss modulus of α and β processes vs annealing temperature. The inset is the ratio of the loss modulus of α- and β-processes with increasing crystalline fraction.

383 K annealed sample were applied in these fittings. The evolution of α- and β-relaxation intensity along with residual glass fraction after annealing at different temperatures is shown in Fig. 9. The intensity of the α process is clearly more strongly correlated to crystallization fraction or glass fraction than the β process. For instance, the intensity of the β relaxation peak retains more than 60% of its original value in the MG composite with less than 20% glass volume fraction, while the corresponding α-relaxation strength drops to ~10% of its initial intensity. This contrast is more apparent when examining the relative β-relaxation intensity (E''_β/E''_α) as a function of crystalline phase fraction, as shown in the inset of Fig. 9. Notably, the dramatic increase of E''_β/E''_α after crystallization makes β relaxation even more prominent and well-separated than in any other fully glassy state of the $Ce_{75}Al_{25}$ alloy. In addition, it is important to note that the β-relaxation peak position remains unchanged across all states, from a fully glassy sample to MG/crystalline composites, indicating the β processes are activated at essentially the same temperature, regardless of the degree of crystallization or changes in glass structure/energy state.

Several models have been proposed to describe the structural characteristics related to β relaxation. According to one of the most widely accepted heterogeneous models of MG atomic structure, consisting of soft "liquid-like" regions (with more free-volume) and hard "solidlike" regions (with less free-volume), it is suggested that atomic rearrangements responsible for β relaxation occur primarily in the soft regions [7–9]. A long-standing controversial question is whether β relaxation involves all atoms in a glass or only a small fraction [72–75]. In a numerical simulation of dynamic shear modulus, the β-wing signal was suppressed when a small fraction of particles was pinned to prevent them from participating in relaxation dynamics, indicating that the β-relaxation process must be cooperative rather than local [76]. However, the dynamic-structure correspondence revealed by the correlation between the characteristic relaxation times τ_β (from sub-T_g enthalpy relaxation) and τ_ξ (from evolution of spatial heterogeneity) provides evidence for the locality of β relaxation [75].

In our work, the prominent β-peak (~60% compared with the fully amorphous state) that remains in the $Ce_{75}Al_{25}$ composite with a crystallization volume fraction exceeding 80% indicates that β relaxation in $Ce_{75}Al_{25}$ MG is much less sensitive to the volume fraction decrease of glass phases. This observation implies that β relaxation may only involve a small subset of atoms and is probably less cooperative than expected in some model glasses discussed before in simulations [74]. Alternative mechanisms, however, may also account for the observed relationship between β relaxation and crystallization, and further microstructural analyses will be needed to resolve this question in the future.

As mentioned above, the β-relaxation peak, which becomes more separated with the weakening of α relaxation in Fig. 7, shows an unchanged position. We modulate the atomic ratio of the Ce-Al MGs to see whether it still holds in other Ce-Al binary MGs. Fig. 10 shows normalized E'' for the Ce-Al MGs and their partial crystallized composites. It is obvious that only the β-peak of the $Ce_{75}Al_{25}$ MG displays no temperature shift after partial crystallization. As shown in Fig. S5 [54], the $Ce_{75}Al_{25}$ MG has one single polymorphic crystalline phase, *hcp*-Ce_3Al, the composition of which is the same as the $Ce_{75}Al_{25}$ MG matrix. Thus the unchanged β-relaxation peak for $Ce_{75}Al_{25}$ composites is due to the identical composition of the remaining glass matrix before and after crystallization. It is the unique polymorphic crystallization characteristic that differs $Ce_{75}Al_{25}$ from other Ce-Al MGs. In the other three Ce-Al MGs, at least two crystalline phases coexist. Therefore the partial crystallization will inevitably change the composition of the remaining MG matrix. Moreover, the shifting directions of the β-relaxation peak after partial crystallization are directly correlated with the crystalline phases. Specifically, the formation of cubic-Ce or hexagonal-Ce in $Ce_{70}Al_{30}$ and $Ce_{65}Al_{35}$ MGs shifts the β-relaxation peaks to a lower temperature regime, while the formation of cubic-Al shifts it to a higher temperature, which changes the relative Ce/Al ratio in the remaining MG matrix. Higher content of Ce in the Ce-Al MG seems to account for the higher temperature β-relaxation peak. Thus the compositional effect is the main factor in shifting the β-relaxation peak position in this Ce-Al MG system. Polymorphic crystallization also exists in binary $Co_{33}Zr_{67}$ [77], $Ti_{67}Ni_{33}$ [78], $Cu_{33}Zr_{67}$ [79], and metal-metalloid $Fe_{66}Ni_{10}B_{24}$ [80] glasses. Unfortunately, none of them shows a prominent β-relaxation peak, therefore, $Ce_{75}Al_{25}$ MG provides a valuable model system to clarify the crystallization effect on β relaxation.

Furthermore, the still prominent β-relaxation peak in partially-crystallized $Ce_{75}Al_{25}$ composites with more than 80% crystallinity probably indicates a different relationship between β relaxation and crystallization at high temperature according to the DMS data. If the crystallization nucleation process initiates at the softest site/region where β relaxation occurs, the β-relaxation peak should be severely suppressed. Thus our results may shed new light on our understanding of the relationship between crystallization and β relaxation. It should be noted that the results are based on high-temperature crystallization, i.e., crystallization was achieved by annealing in the supercooled liquid region at temperatures above T_g. This could be the reason for the contradiction between our results

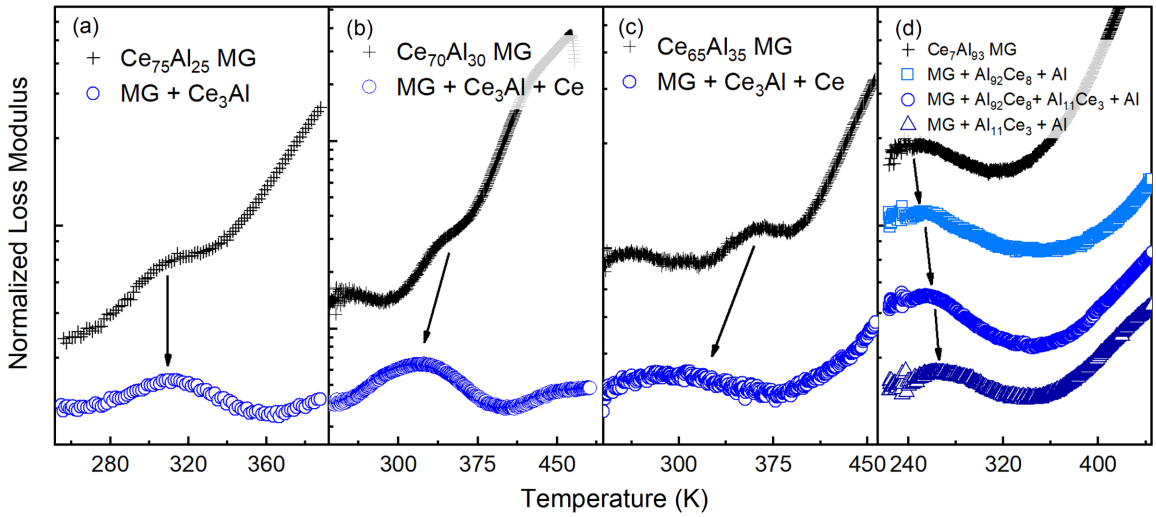

FIG. 10. DMS results of crystallization effects on four Ce-Al MGs with different atomic ratios. (a) $Ce_{75}Al_{25}$. (b) $Ce_{70}Al_{30}$. (c) $Ce_{65}Al_{35}$. (d) Ce_7Al_{93}. The curves are shifted vertically for better comparison. Black arrows mark the shift directions of the β-relaxation peak position.

and former general viewpoints [4,22,23,30], since crystallization in those results was achieved by long-time annealing at low temperatures below T_g.

Kulik [81] has reviewed the effects of annealing conditions on crystallization of MGs, and it was found that two different annealing protocols are applicable for nanocrystallization: very short-time (flash) annealing at high temperatures and long-time annealing at low temperatures. The fact that crystallization could occur well below T_g differs MGs from other amorphous solids (for example, oxide glasses) [82]. To clarify this difference, we compare the DMS data after high-temperature and low-temperature crystallization as shown in Fig. 11. It is surprisingly found that the β-relaxation peak is almost totally suppressed after being annealed at 373 K for ~1000 minutes, while the primary α-relaxation peak is still quite intense, indicating the crystal volume fraction is much lower than being annealed at 443 K for 10 minutes. Hence, the low-temperature annealing results agree well with the general

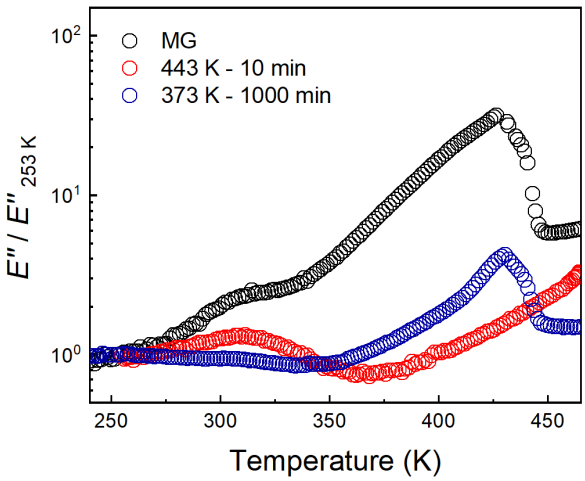

FIG. 11. Comparison of crystallization effects on $Ce_{75}Al_{25}$ MG achieved by annealing at high and low temperatures.

viewpoints that β relaxation governs the nucleation process at relatively low temperatures annealing. While in the supercooled liquid region, β relaxation may depress rather than initiate nucleation of crystals [34]. Therefore, above T_g, crystal nucleation may occur in the β-relaxation inactive regions. These results suggest a totally different role of β relaxation in high-temperature and low-temperature crystallization processes.

Assuming the existence of small quenched-in clusters with short-range order close to a crystalline phase, they can serve as nuclei or sites for heterogeneous nucleation of crystals [81]. In metal-metalloid or transition metal glasses with polymorphic crystallization, it was suggested that for crystallization at low temperatures, particularly at temperatures well below T_g, nucleation occurs heterogeneously and preferentially at the quenched-in nucleation sites; growth rates are controlled by diffusivity, which exhibits an Arrhenius-type temperature dependence. Above T_g, there is strong evidence for a transient homogeneous nucleation process; growth as well as nucleation rates can be described by the VFT equation [82,83].

Thus, combining our results, it is reasonable to infer that the diffusion-controlled crystallization at temperatures below T_g is highly correlated to localized β-relaxation events, leading to similar Arrhenius behavior. The localized soft regions should be spatially linked with the quench-in nucleation sites. A reasonable structural model may be that the "liquidlike" weakly bonded regions are closely surrounded or connected by "solid" quenched-in nuclei. During low-temperature annealing, the local atomic rearrangement of Ce and Al atoms occurs through short-range diffusion in the "liquidlike" soft regions, assisting the growth of surrounding quenched-in nuclei. Above T_g the atomic transport during crystallization is controlled by viscous flow, which could explain the severely suppressed α relaxation in Figs. 7 and 9. It should be noted that microscopic structural characterization with high resolution is essential in the future to confirm such a scenario.

V. CONCLUSION

In summary, after annealing the as-cast $Ce_{75}Al_{25}$ MG ribbons to a well-relaxed "standard" state, we discovered a prominent β-relaxation peak in DMS data, which was not reported in the $Ce_{75}Al_{25}$ MG before. By systematic studies of the influences of physical aging and different thermal treatments on β relaxation of the $Ce_{75}Al_{25}$ MG and its partially crystallized glass-crystal composites, it is revealed that the β relaxation is barely affected by physical aging or other thermal treatment below T_g, which signifies a pseudo JG rather than a genuine JG β relaxation in $Ce_{75}Al_{25}$ MGs, demonstrating the intrinsic thermal stability of the β relaxation. Meanwhile, the relaxation times of physical aging below T_g are well described by MVFT functions, which reveal that aging dynamics at temperatures below T_g, are dominated by α relaxation rather than β relaxation. Crucially, by leveraging the unique polymorphic crystallization of the $Ce_{75}Al_{25}$ MG, we decouple compositional from structural effects, proving that the commonly observed β-relaxation peak shifts in other systems are most likely driven by compositional variations rather than intrinsic structural relaxation. The DMA results of partially-crystallized $Ce_{75}Al_{25}$ MG composites annealed above T_x or below T_g confirm that different crystallization processes have different influences on β relaxation of the MG composites. By separately clarifying the effects of aging and crystallization without interference of noticeable compositional variation, this work helps to resolve long-standing controversies and establishes a new paradigm for better understanding of the α and β relaxations in MGs. Our findings thereby clarify the distinct roles of these relaxation processes in structural and energy evolution, offering a revised conceptual framework for exploring the structure-dynamics relationship in glassy materials.

ACKNOWLEDGMENTS

This research was supported by National Natural Science Foundation of China (Grant No. 52101187) and Shanghai Key Laboratory of Material Frontiers Research in Extreme Environments, China (Grant No. 22dz2260800), and the Shanghai Science and Technology Committee, China (Grant No. 22JC1410300). We thank the Shanghai Synchrotron Radiation Facility of BL15U1 [84] for the assistance on XRD measurements.

DATA AVAILABILITY

The data that support the findings of this article are not publicly available upon publication because it is not technically feasible and/or the cost of preparing, depositing, and hosting the data would be prohibitive within the terms of this research project. The data are available from the authors upon reasonable request.

[1] W. H. Wang, Dynamic relaxations and relaxation-property relationships in metallic glasses, Prog. Mater Sci. **106**, 100561 (2019).

[2] H. S. Chen and N. Morito, Sub-Tgα' relaxation in a PdCuSi glass; internal friction measurements, J. NonCryst. Solids **72**, 287 (1985).

[3] H. Okumura, H. S. Chen, A. Inoue, and T. Masumoto, Structural relaxation of a $La_{55}Al_{25}Ni_{20}$ amorphous alloy measured by an internal friction method, Jpn. J. Appl. Phys. **30**, 2553 (1991).

[4] J. M. Pelletier, B. Van de Moortèle, and I. R. Lu, Viscoelasticity and viscosity of Pd–Ni–Cu–P bulk metallic glasses, Mater. Sci. Eng. A **336**, 190 (2002).

[5] P. Rösner, K. Samwer, and P. Lunkenheimer, Indications for an "excess wing" in metallic glasses from the mechanical loss modulus in $Zr_{65}Al_{7.5}Cu_{27.5}$, Europhys. Lett. **68**, 226 (2004).

[6] Z. F. Zhao, P. Wen, C. H. Shek, and W. H. Wang, Measurements of slow β-relaxataions in metallic glasses and supercooled liquids, Phys. Rev. B **75**, 174201 (2007).

[7] P. Wen, Z. F. Zhao, M. X. Pan, and W. H. Wang, Mechanical relaxation in supercooled liquids of bulk metallic glasses, Phys. Status Solidi A **207**, 2693 (2010).

[8] Z. Wang, K. L. Ngai, and W. H. Wang, Understanding the changes in ductility and Poisson's ratio of metallic glasses during annealing from microscopic dynamics, J. Appl. Phys. **118**, 034901 (2015).

[9] N. B. Olsen, Scaling of β-relaxataion in the equilibrium liquid state of sorbitol, J. NonCryst. Solids **235–237**, 399 (1998).

[10] N. B. Olsen, T. Christensen, and C. J. Dyre, β relaxation of nonpolymeric liquids close to the glass transition, Phys. Rev. E **62**, 4435 (2000).

[11] G. Power, J. K. Vij, and G. P. Johari, Kinetics of spontaneous change in the localized motions of D-sorbitol glass, J. Chem. Phys. **124**, 074509 (2006).

[12] H. Yardimci and R. L. Leheny, Aging of the Johari-Goldstein relaxation in the glass-forming liquids sorbitol and xylitol, J. Chem. Phys. **124**, 214503 (2006).

[13] R. Casalini and C. M. Roland, Aging of the secondary relaxation to probe structural relaxation in the glassy state, Phys. Rev. Lett. **102**, 035701 (2009).

[14] L. C. E. Struik, Effect of thermal history on secondary relaxation processes in amorphous polymers, Polymer **28**, 57 (1987).

[15] E. Muzeau, G. Vigier, and R. Vassoille, Physical aging phenomena in an amorphous polymer at temperatures far below the glass transition, J. NonCryst. Solids **172–174**, 575 (1994).

[16] E. Muzeau, G. Vigier, R. Vassoille, and J. Perez, Changes of thermodynamic and dynamic mechanical properties of poly(methyl methacrylate) due to structural relaxation: Low-temperature ageing and modelling, Polymer **36**, 611 (1995).

[17] K. L. Ngai and M. Paluch, Classification of secondary relaxation in glass-formers based on dynamic properties, J. Chem. Phys. **120**, 857 (2004).

[18] P. Lunkenheimer, R. Wehn, U. Schneider, and A. Loidl, Glassy aging dynamics, Phys. Rev. Lett. **95**, 055702 (2005).

[19] Y. T. Sun, R. Zhao, D. W. Ding, Y. H. Liu, H. Y. Bai, M. Z. Li, and W. H. Wang, Distinct relaxation mechanism at room temperature in metallic glass, Nat. Commun. **14**, 540 (2023).

[20] Y. Zhao, B. Shang, B. Zhang, X. Tong, H. Ke, H. Bai, and W.-H. Wang, Ultrastable metallic glass by room temperature aging, Sci. Adv. **8**, eabn3623 (2022).

[21] C. Tang and P. Harrowell, Anomalously slow crystal growth of the glass-forming alloy CuZr, Nat. Mater. **12**, 507 (2013).
[22] C. Desgranges and J. Delhommelle, Unusual crystallization behavior close to the glass transition, Phys. Rev. Lett. **120**, 115701 (2018).
[23] G. Sun, J. Xu, and P. Harrowell, The mechanism of the ultrafast crystal growth of pure metals from their melts, Nat. Mater. **17**, 881 (2018).
[24] D. C. Hofmann, J. Y. Suh, A. Wiest, G. Duan, M. L. Lind, M. D. Demetriou, and W. L. Johnson, Designing metallic glass matrix composites with high toughness and tensile ductility, Nature (London) **451**, 1085 (2008).
[25] W. Song, Y. Wu, H. Wang, X. Liu, H. Chen, Z. Guo, and Z. Lu, Microstructural control via copious nucleation manipulated by in situ formed nucleants: Large-sized and ductile metallic glass composites, Adv. Mater. **28**, 8156 (2016).
[26] A. Takeuchi, Y. Zhang, K. Takenaka, and A. Makino, Thermodynamic analysis of binary $Fe_{85}B_{15}$ to quinary $Fe_{85}Si_2B_8P_4Cu_1$ alloys for primary crystallizations of α-Fe in nanocrystalline soft magnetic alloys, J. Appl. Phys. **117**, 17b737 (2015).
[27] S. Chen, G. Yang, S. Luo, S. Yin, J. Jia, Z. Li, S. Gao, Y. Shao, and K. Yao, Unexpected high performance of Fe-based nanocrystallized ribbons for azo dye decomposition, J. Mater. Chem. A **5**, 14230 (2017).
[28] T. Hikima, M. Hanaya, and M. Oguni, Numerical and morphological approach to the mechanism of homogeneous-nucleation-based crystallization in o-terphenyl, J. NonCryst. Solids **235–237**, 539 (1998).
[29] M. Hatase, M. Hanaya, T. Hikima, and M. Oguni, Discovery of homogeneous-nucleation-based crystallization in simple glass-forming liquid of toluene below its glass-transition temperature, J. NonCryst. Solids **307–310**, 257 (2002).
[30] F. Paladi and M. Oguni, Anomalous generation and extinction of crystal nuclei in nonequilibrium supercooled liquido-benzylphenol, Phys. Rev. B **65**, 144202 (2002).
[31] K. L. Ngai, *Relaxation and Diffusion in Complex Systems* (Springer, New York, 2011), p. 835.
[32] T. Ichitsubo, E. Matsubara, S. Kai, and M. Hirao, Ultrasound-induced crystallization around the glass transition temperature for $Pd_{40}Ni_{40}P_{20}$ metallic glass, Acta Mater. **52**, 423 (2004).
[33] T. Ichitsubo, E. Matsubara, T. Yamamoto, H. S. Chen, N. Nishiyama, J. Saida, and K. Anazawa, Microstructure of fragile metallic glasses inferred from ultrasound-accelerated crystallization in Pd-based metallic glasses, Phys. Rev. Lett. **95**, 245501 (2005).
[34] L. J. Song, M. Gao, W. Xu, J. T. Huo, J. Q. Wang, R. W. Li, W. H. Wang, and J. H. Perepezko, Inheritance from glass to liquid: β relaxation depresses the nucleation of crystals, Acta Mater. **185**, 38 (2020).
[35] H. B. Yu, K. Samwer, W. H. Wang, and H. Y. Bai, Chemical influence on β-relaxataions and the formation of molecule-like metallic glasses, Nat. Commun. **4**, 2204 (2013).
[36] Z. G. Zhu, Z. Wang, and W. H. Wang, Binary rare earth element-Ni/Co metallic glasses with distinct β-relaxataion behaviors, J. Appl. Phys. **118**, 154902 (2015).
[37] Q. S. Zeng, Y. Ding, W. L. Mao, W. Yang, S. V. Sinogeikin, J. Shu, H. K. Mao, and J. Z. Jiang, Origin of pressure-induced polyamorphism in $Ce_{75}Al_{25}$ metallic glass, Phys. Rev. Lett. **104**, 105702 (2010).
[38] Q. Zeng, H. Sheng, Y. Ding, L. Wang, W. Yang, J.-Z. Jiang, L. Mao Wendy, and H.-K. Mao, Long-range topological order in metallic glass, Science **332**, 1404 (2011).
[39] M. Wu, J. S. Tse, S. Y. Wang, C. Z. Wang, and J. Z. Jiang, Origin of pressure-induced crystallization of $Ce_{75}Al_{25}$ metallic glass, Nat. Commun. **6**, 6493 (2015).
[40] J. Hachenberg, D. Bedorf, K. Samwer, R. Richert, A. Kahl, M. D. Demetriou, and W. L. Johnson, Merging of the α and β relaxations and aging via the Johari–Goldstein modes in rapidly quenched metallic glasses, Appl. Phys. Lett. **92**, 131911 (2008).
[41] E. Pineda, P. Bruna, B. Ruta, M. Gonzalez-Silveira, and D. Crespo, Relaxation of rapidly quenched metallic glasses: Effect of the relaxation state on the slow low temperature dynamics, Acta Mater. **61**, 3002 (2013).
[42] X. D. Wang, B. Ruta, L. H. Xiong, D. W. Zhang, Y. Chushkin, H. W. Sheng, H. B. Lou, Q. P. Cao, and J. Z. Jiang, Free-volume dependent atomic dynamics in beta relaxation pronounced La-based metallic glasses, Acta Mater. **99**, 290 (2015).
[43] S. Havriliak and S. Negami, A complex plane representation of dielectric and mechanical relaxation processes in some polymers, Polymer **8**, 161 (1967).
[44] H. B. Yu, W. H. Wang, H. Y. Bai, and K. Samwer, The β-relaxataion in metallic glasses, Natl. Sci. Rev. **1**, 429 (2014).
[45] Q. Wang, S. T. Zhang, Y. Yang, Y. D. Dong, C. T. Liu, and J. Lu, Unusual fast secondary relaxation in metallic glass, Nat. Commun. **6**, 7876 (2015).
[46] G. S. Fulcher, Analysis of recent measurements of the viscosity of glasses, J. Am. Ceram. Soc. **8**, 339 (1925).
[47] S. Havriliak and S. J. Havriliak, Comparison of the Havriliak-Negami and stretched exponential functions, Polymer **37**, 4107 (1996).
[48] J. Qiao, J. M. Pelletier, and R. Casalini, Relaxation of bulk metallic glasses studied by mechanical spectroscopy, J. Phys. Chem. B **117**, 13658 (2013).
[49] J. Qiao, R. Casalini, J. M. Pelletier, and H. Kato, Characteristics of the structural and Johari-Goldstein relaxations in Pd-based metallic glass-forming liquids, J. Phys. Chem. B **118**, 3720 (2014).
[50] M. L. Williams, R. F. Landel, and J. D. Ferry, The temperature dependence of relaxation mechanisms in amorphous polymers and other glass-forming liquids, J. Am. Chem. Soc. **77**, 3701 (1955).
[51] K. Schröter, G. Wilde, R. Willnecker, M. Weiss, K. Samwer, and E. Donth, Shear modulus and compliance in the range of the dynamic glass transition for metallic glasses, Eur. Phys. J. B **5**, 1 (1998).
[52] J. C. Qiao, Q. Wang, J. M. Pelletier, H. Kato, R. Casalini, D. Crespo, E. Pineda, Y. Yao, and Y. Yang, Structural heterogeneities and mechanical behavior of amorphous alloys, Prog. Mater Sci. **104**, 250 (2019).
[53] L.-M. Wang, R. Liu, and W. H. Wang, Relaxation time dispersions in glass forming metallic liquids and glasses, J. Chem. Phys. **128**, 164503 (2008).
[54] See Supplemental Material at http://link.aps.org/supplemental/10.1103/1b87-ycj2 for Figs. S1-S5.
[55] Y. J. Duan, M. Nabahat, Y. Tong, L. Ortiz-Membrado, E. Jiménez-Piqué, K. Zhao, Y.-J. Wang, Y. Yang, T. Wada, H. Kato *et al.*, Connection between mechanical relaxation and equilibra-

tion kinetics in a high-entropy metallic glass, Phys. Rev. Lett. **132**, 056101 (2024).
[56] L. C. E. Struik, *Physical Aging in Amorphous Polymers and Other Materials* (Elsevier Scientific Publishing Company, Amsterdam, 1978).
[57] J. Qiao, R. Casalini, and J. M. Pelletier, Effect of physical aging on Johari-Goldstein relaxation in La-based bulk metallic glass, J. Chem. Phys. **141**, 104510 (2014).
[58] G. P. Johari, Effect of annealing on the secondary relaxations in glasses, J. Chem. Phys. **77**, 4619 (1982).
[59] B. Ruta, Y. Chushkin, G. Monaco, L. Cipelletti, E. Pineda, P. Bruna, V. M. Giordano, and M. Gonzalez-Silveira, Atomic-scale relaxation dynamics and aging in a metallic glass probed by x-ray photon correlation spectroscopy, Phys. Rev. Lett. **109**, 165701 (2012).
[60] M. Frey, R. Busch, W. Possart, and I. Gallino, On the thermodynamics, kinetics, and sub-T_g relaxations of Mg-based bulk metallic glasses, Acta Mater. **155**, 117 (2018).
[61] A. van den Beukel and J. Sietsma, The glass transition as a free volume related kinetic phenomenon, Acta Metall. Mater. **38**, 383 (1990).
[62] R. Busch, E. Bakke, and W. L. Johnson, Viscosity of the supercooled liquid and relaxation at the glass transition of the $Zr_{46.75}Ti_{8.25}Cu_{7.5}Ni_{10}Be_{27.5}$ bulk metallic glass forming alloy, Acta Mater. **46**, 4725 (1998).
[63] A. R. Yavari, A. L. Moulec, A. Inoue, N. Nishiyama, N. Lupu, E. Matsubara, W. J. Botta, G. Vaughan, M. D. Michiel, and Å. Kvick, Excess free volume in metallic glasses measured by X-ray diffraction, Acta Mater. **53**, 1611 (2005).
[64] S. V. Ketov, Y. H. Sun, S. Nachum, Z. Lu, A. Checchi, A. R. Beraldin, H. Y. Bai, W. H. Wang, D. V. Louzguine-Luzgin, M. A. Carpenter *et al.*, Rejuvenation of metallic glasses by non-affine thermal strain, Nature (London) **524**, 200 (2015).
[65] Q. Zeng, In situ high-pressure wide-angle hard x-ray photon correlation spectroscopy: A versatile tool probing atomic dynamics of extreme condition matter, Matter Radiat. Extrem. **8**, 028101 (2023).
[66] X. Zhang, H. Lou, B. Ruta, Y. Chushkin, F. Zontone, S. Li, D. Xu, T. Liang, Z. Zeng, H.-k. Mao *et al.*, Pressure-induced nonmonotonic cross-over of steady relaxation dynamics in a metallic glass, Proc. Natl Acad. Sci. USA **120**, e2302281120 (2023).
[67] U. Schneider, R. Brand, P. Lunkenheimer, and A. Loidl, Excess wing in the dielectric loss of glass formers: A Johari-Goldstein β relaxation? Phys. Rev. Lett. **84**, 5560 (2000).
[68] L. T. Zhang, J. M. Pelletier, and J. C. Qiao, Dynamic mechanical behavior of $(La_{0.7}Ce_{0.3})_{65}Al_{10}Co_{25}$ bulk metallic glass: Influence of the physical aging and heat treatment, J. Alloys Compd. **869**, 159271 (2021).
[69] D. Cangialosi, M. Wübbenhorst, H. Schut, A. van Veen, and S. J. Picken, Dynamics of polycarbonate far below the glass transition temperature: A positron annihilation lifetime study, Phys. Rev. B **69**, 134206 (2004).
[70] I. M. Hodge, Adam-Gibbs formulation of nonlinearity in glassy-state relaxations, Macromolecules **19**, 936 (1986).
[71] M. Hodge Ian, Physical aging in polymer glasses, Science **267**, 1945 (1995).
[72] G. P. Johari and M. Goldstein, Viscous liquids and the glass transition. II. secondary relaxations in glasses of rigid molecules, J. Chem. Phys. **53**, 2372 (1970).
[73] H. B. Yu, K. Samwer, Y. Wu, and W. H. Wang, Correlation between beta relaxation and self-diffusion of the smallest constituting atoms in metallic glasses, Phys. Rev. Lett. **109**, 095508 (2012).
[74] S. Karmakar, C. Dasgupta, and S. Sastry, Short-time beta relaxation in glass-forming liquids is cooperative in nature, Phys. Rev. Lett. **116**, 085701 (2016).
[75] F. Zhu, H. K. Nguyen, S. X. Song, D. P. Aji, A. Hirata, H. Wang, K. Nakajima, and M. W. Chen, Intrinsic correlation between β-relaxataion and spatial heterogeneity in a metallic glass, Nat. Commun. **7**, 11516 (2016).
[76] Y. Cohen, S. Karmakar, I. Procaccia, and K. Samwer, The nature of the β-peak in the loss modulus of amorphous solids, Europhys. Lett. **100**, 36003 (2012).
[77] U. Köster and M. Blank-Bewersdorff, Transient nucleation in Co-Zr metallic glasses, OPL **57**, 115 (1985).
[78] M. Buchwitz, R. Adlwarth-Dieball, and P. L. Ryder, Kinetics of the crystallization of amorphous Ti_2Ni, Acta Metall. Mater. **41**, 1885 (1993).
[79] Y.-H. Jiang, D. Li, F. Liu, and S.-H. Liang, Crystallization kinetics of $Cu_{33}Zr_{67}$ amorphous alloy during continuous cooling annealing, Mater. Lett. **181**, 292 (2016).
[80] U. Köster, U. Schünemann, M. Blank-Bewersdorff, S. Brauer, M. Sutton, and G. B. Stephenson, Nanocrystalline materials by crystallization of metal-metalloid glasses, Mater. Sci. Eng. A **133**, 611 (1991).
[81] T. Kulik, Nanocrystallization of metallic glasses, J. NonCryst. Solids **287**, 145 (2001).
[82] U. Köster and J. Meinhardt, Crystallization of highly undercooled metallic melts and metallic glasses around the glass transition temperature, Mater. Sci. Eng. A **178**, 271 (1994).
[83] A. L. Greer, Crystallization of amorphous alloys, Metall. Mater. Trans. A **27**, 549 (1996).
[84] https://cstr.cn/31124.02.SSRF.BL15U1.